

Effects of Thermal Radiation on Unsteady Magnetohydrodynamic Flow of a Micropolar Fluid with Heat and Mass Transfer

Tasawar Hayat^{a,b} and Muhammad Qasim^a

^a Department of Mathematics, Quaid-I-Azam University 45320, Islamabad 44000, Pakistan

^b Department of Mathematics, College of Sciences, King Saud University, P. O. Box 2455, Riyadh 11451, Saudi Arabia

Reprint requests to T. H.; E-mail: pensy_t@yahoo.com

Z. Naturforsch. **65a**, 950–960 (2010); received November 17, 2009 / revised February 21, 2010

An analysis has been carried out to study the combined effects of heat and mass transfer on the unsteady flow of a micropolar fluid over a stretching sheet. The thermal radiation effects are presented. The arising nonlinear partial differential equations are first reduced to a set of nonlinear ordinary differential equations and then solved by the homotopy analysis method (HAM). Plots for various interesting parameters are presented and discussed. Numerical data for surface shear stress, Nusselt number, and Sherwood number in steady case are also tabulated. Comparison between the present and previous limiting results is given.

Key words: Unsteady Flow; Micropolar Fluid; MHD Flow; Mass Transfer.

1. Introduction

There exist many fluids in industry and engineering which cannot be interpreted by a linear relationship between stress and deformation rate. Such fluids are called the non-Newtonian fluids. Examples of such fluids are molten polymers, pulps, foods, fossil fuels, muds, fluids containing certain additives, and some naturally occurring fluids such as animal blood. However, the non-Newtonian fluids cannot be studied by employing a single constitutive relationship. This is due to diverse properties of non-Newtonian fluids in nature. Hence many models of non-Newtonian fluids have been reported. Amongst the several models of non-Newtonian fluids [1–18], the micropolar fluids have attracted much attention from the researchers. This is due to the fact that the equations governing the flow of a micropolar fluid involve a microrotation vector and a gyration parameter in addition to the classical velocity vector field. Nazar et al. [19] described the steady stagnation point flow of an incompressible fluid bounded by a stretched sheet in its own plane. Axisymmetric flow of a micropolar fluid between two porous disks with heat transfer is examined by Takhar et al. [20]. They presented the finite element solution. Chang [21] provided a numerical analysis for mixed convection flow in a micropolar fluid flowing along a vertical flat plate. Gorla [22] analyzed the thermal

boundary layer of a micropolar fluid in the vicinity of a stagnation point. Abo-Eldahab and Aziz [23] studied the heat transfer effects on the flow of a micropolar fluid past a stretched sheet embedded in a non-Darcian medium. The flow problem of a micropolar fluid induced by the rotary oscillations of two concentric spheres has been analyzed by Iyengar and Vani [24]. The arterial flow in the presence of stenosis has been examined by Philip and Chandra [25]. They treated blood as a micropolar fluid. Blasius flow problem as a micropolar fluid is numerically discussed by Rees and Bossom [26]. Hayat et al. [27] studied the stagnation point flow of a micropolar fluid towards a nonlinear stretching sheet in the presence of an uniform applied magnetic field. Non-similar solutions for the boundary layers on a sphere in a micropolar fluid with heat and mass fluxes have been reported by Cheng [28]. Eldabe and Ouaf [29] looked at the heat and mass transfer effects on the stretching flow of a micropolar fluid in the presence of Ohmic heating and viscous dissipation.

The boundary layer flows of a non-Newtonian fluid over a stretching sheet are always important from engineering point of view. For example in extrusion process, glass fiber and paper production, wire drawing, food processing, and movement of biological fluids. Very recently, Nazar et al. [30] looked at the unsteady flow over a stretching sheet in a micropolar fluid. The heat transfer analysis of a boundary layer flow with

radiation is further important in electrical power generation, astrophysical flows, solar power technology, space vehicle re-entry, and other industrial areas. Mass transfer in the boundary layer flow is also an interesting topic of research with a wide range of applications. This is significant in membrane separation process microfiltration, reverse osmosis, and has considerable practical relevance, e. g. in electrochemistry, in fiber industries, and other physical problems in which fluids undergo exothermic and endothermic chemical reactions.

The aim of the current study is to extend the analysis of [30] in four directions. Firstly to discuss the MHD effects. Secondly to analyze the heat transfer effects in presence of a thermal radiation. Thirdly to describe the influence of mass transfer. Fourthly to perform computation for the homotopy solutions. The homotopy analysis method (HAM) proposed by Liao [31] is used for the development of series solutions. This method is very powerful and has been already applied by many investigators [32–46].

2. Mathematical Formulation

We investigate the unsteady flow of a micropolar fluid over a stretching surface. The fluid is electrically conducting in the presence of a constant applied magnetic field B_0 . The induced magnetic field is neglected under the assumption of a small magnetic Reynold number [47]. Initially (for $t = 0$), both fluid and plate are stationary. The fluid has constant temperature T_∞ and concentration C_∞ . The plate at $y = 0$ is stretched by the velocity component $u = ax$. For $t > 0$ the surface temperature and concentration are T_w and C_w , respectively. The boundary layer flow is governed by the following equations:

$$\frac{\partial u}{\partial x} + \frac{\partial v}{\partial y} = 0, \tag{1}$$

$$\frac{\partial u}{\partial t} + u \frac{\partial u}{\partial x} + v \frac{\partial u}{\partial y} = \left(\nu + \frac{\kappa}{\rho} \right) \frac{\partial^2 u}{\partial y^2} + \frac{\kappa}{\rho} \frac{\partial N}{\partial y} - \frac{\sigma B_0^2}{\rho} u, \tag{2}$$

$$\frac{\partial N}{\partial t} + u \frac{\partial N}{\partial x} + v \frac{\partial N}{\partial y} = \frac{\gamma^*}{\rho j} \frac{\partial^2 N}{\partial y^2} - \frac{\kappa}{\rho j} \left(2N + \frac{\partial u}{\partial y} \right), \tag{3}$$

$$\rho c_p \left[\frac{\partial T}{\partial t} + u \frac{\partial T}{\partial x} + v \frac{\partial T}{\partial y} \right] = k \frac{\partial^2 T}{\partial y^2} - \frac{\partial q_r}{\partial y}, \tag{4}$$

$$\frac{\partial C}{\partial t} + u \frac{\partial C}{\partial x} + v \frac{\partial C}{\partial y} = D \frac{\partial^2 C}{\partial y^2} - k_1 C, \tag{5}$$

and the subjected conditions are

$$\begin{aligned} u = v = N = 0, \quad T = T_\infty, \quad C = C_\infty, \quad t < 0, \\ u = u_w = ax, \quad v = 0, \quad N = -m_0 \frac{\partial u}{\partial y}, \quad T = T_w, \\ C = C_w, \quad y = 0; \quad t \geq 0, \quad u \rightarrow 0, \quad v \rightarrow 0, \\ N \rightarrow 0, \quad T \rightarrow 0, \quad C \rightarrow 0, \quad \text{as } y \rightarrow \infty, \end{aligned} \tag{6}$$

where in (4) the viscous dissipation is not included. In above equations u and v are the velocity components along the x - and y -axes, respectively, ρ is the fluid density, ν the kinematic viscosity, σ the electrical conductivity, N the microrotation or angular velocity, T the temperature, c_p the specific heat, k the thermal conductivity of the fluid, q_r the radiative heat flux, C is the concentration species of the fluid, D the diffusion coefficient of the diffusion species in the fluid, k_1 denotes the first-order homogeneous constant reaction rate, $j = (\nu/c)$ is the microinertia per unit mass, $\gamma^* = (\mu + \kappa/2)j$ and κ are the spin gradient viscosity and vortex viscosity, respectively. Here m_0 is a constant and $0 \leq m_0 \leq 1$. The case $m_0 = 0$, which indicates $N = 0$ at the wall, represents concentrated particle flows in which the microelements close to the wall surface are unable to rotate [1]. This case is also known as the strong concentration of mircoelements [2]. The case $m_0 = \frac{1}{2}$ indicates the vanishing of the anti-symmetric part of the stress tensor and denotes weak concentration [3] of mircoelements. We shall consider here both cases of $m_0 = 0$ and $m_0 = \frac{1}{2}$. However, it can easily be shown that for $m_0 = \frac{1}{2}$ the governing equations can be reduced to the classical problem of steady boundary layer flow of a viscous incompressible fluid near the plane wall. However, the most common boundary condition used in the literature is the vanishing of the spin on the boundary, so-called strong interaction. The opposite extreme, the weak interaction, is the vanishing of the momentum stress on the boundary [2]. A third or compromise in the vanishing of a linear combination of spin, shearing stress and couple stress, involving some friction coefficients, a particular case of which was the condition used by Peddieson [4].

Employing Rosseland approximation we have

$$q_r = - \frac{4\sigma^*}{3k^*} \frac{\partial T^4}{\partial y}, \tag{7}$$

where σ^* is the Stefan–Boltzmann constant and k^* the mean absorption coefficient. Using Taylor series one

can expand from T^4 about T_∞ as

$$T^4 \cong 4T_\infty^3 T - 3T_\infty^4, \tag{8}$$

where the higher-order terms have been neglected.

Now with (4), (7), and (8) we have

$$\begin{aligned} &\rho c_p \left[\frac{\partial T}{\partial t} + u \frac{\partial T}{\partial x} + v \frac{\partial T}{\partial y} \right] \\ &= \frac{\partial}{\partial y} \left[\left(\frac{16\sigma^* T_\infty^3}{3k^*} + k \right) \frac{\partial T}{\partial y} \right]. \end{aligned} \tag{9}$$

Defining

$$\begin{aligned} \psi &= (a\nu)^{1/2} \xi^{1/2} x f(\xi, \eta), \\ N &= (a/\nu)^{1/2} \xi^{-1/2} a x g(\xi, \eta), \\ \eta &= (a/\nu)^{1/2} \xi^{-1/2} y, \quad \xi = 1 - \exp(-\tau), \\ \tau &= at, \quad \theta = \frac{T - T_\infty}{T_w - T_\infty}, \quad \phi = \frac{C - C_\infty}{C_w - C_\infty}. \end{aligned} \tag{10}$$

Then (1) is automatically satisfied and (2), (3), (5), (6), and (9) reduce to

$$(1 + K)f''' + (1 - \xi) \left(\frac{\eta}{2} f'' - \xi \frac{\partial f'}{\partial \xi} \right) \tag{11}$$

$$+ \xi [f f'' - (f')^2 - M^2 f'] + K g' = 0,$$

$$\left(1 + \frac{K}{2} \right) g'' + (1 - \xi) \left(\frac{1}{2} g + \frac{\eta}{2} g' - \xi \frac{\partial g}{\partial \xi} \right) \tag{12}$$

$$+ \xi [f g' - f' g - 2K g - K f''] = 0,$$

$$(1 + N_R)\theta'' + Pr(1 - \xi) \left(\frac{\eta}{2} \theta' - \xi \frac{\partial \theta}{\partial \xi} \right) \tag{13}$$

$$+ Pr \xi f \theta' = 0,$$

$$\phi'' + Sc(1 - \xi) \left(\frac{\eta}{2} \phi' - \xi \frac{\partial \phi}{\partial \xi} \right) + Sc \xi f \phi' \tag{14}$$

$$- \gamma Sc \xi \phi = 0,$$

$$f(\xi, 0), f'(\xi, 0) = 1, g(\xi, 0) = -m_0 f''(\xi, 0),$$

$$\theta(\xi, 0) = \phi(\xi, 0) = 1, \tag{15}$$

$$f'(\xi, \infty) = g(\xi, \infty) = \theta(\xi, \infty) = \phi(\xi, \infty) = 0,$$

where a prime denotes the derivative with respect to η . Here material parameter K , Hartman number M , Prandtl number Pr , radiation parameter N_R , Schmidt number Sc , and chemical reaction parameter γ are given by

$$K = \frac{\kappa}{\mu}, \quad M^2 = \frac{\sigma B_0^2}{\rho a}, \quad Pr = \frac{\mu c_p}{k}, \tag{16}$$

$$N_R = \frac{16\sigma^* T_\infty^3}{3kk^*}, \quad Sc = \frac{\nu}{D}, \quad \gamma = \frac{k_1}{a}.$$

The skin friction coefficients C_{fx} , local Nusselt number Nu , and local Sherwood number Sh are defined by the following expressions:

$$C_{fx} = \frac{\left[(\mu + \kappa) \frac{\partial u}{\partial y} + \kappa N \right]_{y=0}}{\rho u_w^2}, \tag{17}$$

$$Nu = \frac{-x(\partial T / \partial y)_{y=0}}{(T_w - T_\infty)}, \quad Sh = \frac{-x(\partial C / \partial y)_{y=0}}{(C_w - C_\infty)}.$$

Utilizing (10) we obtain

$$Re_x^{1/2} \xi^{1/2} C_{fx} = [1 + (1 - m_0)K] f''(\xi, 0),$$

$$Nu Re_x^{-1/2} \xi^{1/2} = -\theta'(\xi, 0), \tag{18}$$

$$Sh Re_x^{-1/2} \xi^{1/2} = -\phi'(\xi, 0),$$

where $Re_x = ax^2/\nu$ is the local Reynolds number.

For $\xi = 0$ (initial unsteady-state flow), (11)–(14) can be written as

$$(1 + K)f''' + \frac{\eta}{2} f'' + K g' = 0, \tag{19a}$$

$$\left(1 + \frac{K}{2} \right) g'' + \frac{\eta}{2} g' + \frac{1}{2} g = 0, \tag{19b}$$

$$(1 + N_R)\theta'' + Pr \frac{\eta}{2} \theta' = 0, \tag{19c}$$

$$\phi'' + Sc \frac{\eta}{2} \phi' = 0. \tag{19d}$$

When $\xi = 1$ (final steady state flow) then (11)–(14) become

$$(1 + K)f''' + f f'' - (f')^2 - M^2 f' + K g' = 0, \tag{20a}$$

$$\left(1 + \frac{K}{2} \right) g'' + f g' - f' g - 2K g - K f'' = 0, \tag{20b}$$

$$(1 + N_R)\theta'' + Pr f \theta' = 0, \tag{20c}$$

$$\phi'' + Sc f \phi' - \gamma Sc \phi = 0. \tag{20d}$$

3. Homotopy Analysis Solutions

To get the homotopy analysis solutions, we substitute $f(\xi, \eta)$, $g(\xi, \eta)$, $\theta(\xi, \eta)$, and $\phi(\xi, \eta)$ by a set of base functions

$$\{ \xi^k \eta^j \exp(-n\eta) \mid k \geq 0, n \geq 0, j \geq 0 \}$$

in the form

$$f(\eta, \xi) = a_{0,0}^0 + \sum_{k=0}^{\infty} \sum_{j=0}^{\infty} \sum_{n=1}^{\infty} a_{j,n}^k \xi^k \eta^j \exp(-n\eta), \quad (21)$$

$$g(\eta, \xi) = \sum_{k=0}^{\infty} \sum_{j=0}^{\infty} \sum_{n=1}^{\infty} b_{j,n}^k \xi^k \eta^j \exp(-n\eta), \quad (22)$$

$$\theta(\eta, \xi) = \sum_{k=0}^{\infty} \sum_{j=0}^{\infty} \sum_{n=1}^{\infty} c_{j,n}^k \xi^k \eta^j \exp(-n\eta), \quad (23)$$

$$\phi(\eta, \xi) = \sum_{k=0}^{\infty} \sum_{j=0}^{\infty} \sum_{n=1}^{\infty} d_{j,n}^k \xi^k \eta^j \exp(-n\eta), \quad (24)$$

in which $a_{j,n}^k, b_{j,n}^k, c_{j,n}^k,$ and $d_{j,n}^k$ are the coefficients. By the rule of solution expressions and with the boundary conditions (15), we can choose the initial guesses $f_0, g_0, \theta_0,$ and ϕ_0 of $f(\xi, \eta), g(\xi, \eta), \theta(\xi, \eta),$ and $\phi(\xi, \eta)$ as follows:

$$f_0(\xi, \eta) = 1 - \exp(-\eta), \quad (25)$$

$$g_0(\xi, \eta) = m_0 \exp(-\eta), \quad (26)$$

$$\theta_0(\xi, \eta) = \exp(-\eta), \quad (27)$$

$$\phi_0(\xi, \eta) = \exp(-\eta). \quad (28)$$

The auxiliary linear operators are defined by the following equations:

$$\mathcal{L}_f = \frac{d^3 f}{d\eta^3} - \frac{df}{d\eta}, \quad (29)$$

$$\mathcal{L}_g = \frac{d^2 g}{d\eta^2} - g, \quad (30)$$

$$\mathcal{L}_\theta = \frac{d^2 \theta}{d\eta^2} - \theta, \quad (31)$$

$$\mathcal{L}_\phi = \frac{d^2 \phi}{d\eta^2} - \phi, \quad (32)$$

which satisfy

$$\mathcal{L}_f [C_1 + C_2 \exp(\eta) + C_3 \exp(-\eta)] = 0, \quad (33)$$

$$\mathcal{L}_g [C_4 \exp(\eta) + C_5 \exp(-\eta)] = 0, \quad (34)$$

$$\mathcal{L}_\theta [C_6 \exp(\eta) + C_7 \exp(-\eta)] = 0, \quad (35)$$

$$\mathcal{L}_\phi [C_8 \exp(\eta) + C_9 \exp(-\eta)] = 0, \quad (36)$$

where $C_i (i = 1 - 9)$ are arbitrary constants.

If $p \in [0, 1]$ denotes the embedding parameter and $\hbar_f, \hbar_g, \hbar_\theta,$ and \hbar_ϕ the non-zero auxiliary parameters,

then we construct the zeroth-order deformation equations

$$(1 - p)\mathcal{L}_f[\hat{f}(\xi, \eta; p) - f_0(\xi, \eta)] = p\hbar_f \mathcal{N}_f[\hat{f}(\xi, \eta; p)], \quad (37)$$

$$(1 - p)\mathcal{L}_g[\hat{g}(\xi, \eta; p) - g_0(\xi, \eta)] = p\hbar_g \mathcal{N}_g[\hat{f}(\xi, \eta; p), \hat{g}(\xi, \eta; p)], \quad (38)$$

$$(1 - p)\mathcal{L}_\theta[\hat{\theta}(\xi, \eta; p) - \theta_0(\xi, \eta)] = p\hbar_\theta \mathcal{N}_\theta[\hat{f}(\xi, \eta; p), \hat{\theta}(\xi, \eta; p)], \quad (39)$$

$$(1 - p)\mathcal{L}_\phi[\hat{\phi}(\xi, \eta; p) - \phi_0(\xi, \eta)] = p\hbar_\phi \mathcal{N}_\phi[\hat{f}(\xi, \eta; p), \hat{\phi}(\xi, \eta; p)], \quad (40)$$

subjected to the following boundary conditions:

$$\hat{f}(\eta; \xi)|_{\eta=0} = 0,$$

$$\hat{g}(\eta; \xi)|_{\eta=0} = -m_0 \frac{\partial^2 \hat{f}(\eta; \xi)}{\partial \eta^2} \Big|_{\eta=0},$$

$$\hat{\theta}(\eta; \xi)|_{\eta=0} = \hat{\phi}(\eta; \xi)|_{\eta=0} = \frac{\partial \hat{f}(\eta; \xi)}{\partial \eta} \Big|_{\eta=0} = 1, \quad (41)$$

$$\hat{g}(\eta; \xi)|_{\eta=\infty} = 0,$$

$$\frac{\partial \hat{f}(\eta; \xi)}{\partial \eta} \Big|_{\eta=\infty} = \hat{\theta}(\eta; \xi)|_{\eta=\infty} = \hat{\phi}(\eta; \xi)|_{\eta=\infty} = 0,$$

in which we define the nonlinear operators $\mathcal{N}_f, \mathcal{N}_g, \mathcal{N}_\theta,$ and \mathcal{N}_ϕ as

$$\begin{aligned} \mathcal{N}_f[\hat{f}(\xi, \eta; p), \hat{g}(\xi, \eta; p)] &= (1 + K) \frac{\partial^3 \hat{f}(\xi, \eta; p)}{\partial \eta^3} \\ &+ (1 - \xi) \left(\frac{\eta}{2} \frac{\partial^2 \hat{f}(\xi, \eta; p)}{\partial \eta^2} - \xi \frac{\partial^2 \hat{f}(\xi, \eta; p)}{\partial \eta \partial \xi} \right) \\ &+ \xi \left[\hat{f}(\xi, \eta; p) \frac{\partial^2 \hat{f}(\xi, \eta; p)}{\partial \eta^2} - \left(\frac{\partial \hat{f}(\xi, \eta; p)}{\partial \eta} \right)^2 \right. \\ &\left. - M^2 \frac{\partial \hat{f}(\xi, \eta; p)}{\partial \eta} \right] + Kg', \end{aligned} \quad (42)$$

$$\begin{aligned} \mathcal{N}_g[\hat{f}(\xi, \eta; p), \hat{g}(\xi, \eta; p)] &= \left(1 + \frac{K}{2} \right) \frac{\partial^2 \hat{g}(\xi, \eta; p)}{\partial \eta^2} \\ &+ (1 - \xi) \left(\frac{\eta}{2} \frac{\partial \hat{g}(\xi, \eta; p)}{\partial \eta} - \xi \frac{\partial \hat{g}(\xi, \eta; p)}{\partial \xi} \right) \\ &+ \frac{1}{2} \hat{g}(\xi, \eta; p) + \xi \left[\hat{f}(\xi, \eta; p) \frac{\partial \hat{g}(\xi, \eta; p)}{\partial \eta} \right. \\ &\left. - \hat{f}(\xi, \eta; p) \frac{\partial \hat{g}(\xi, \eta; p)}{\partial \eta} - 2K\hat{g}(\xi, \eta; p) \right. \\ &\left. - K \frac{\partial^2 \hat{f}(\xi, \eta; p)}{\partial \eta^2} \right], \end{aligned} \quad (43)$$

$$\begin{aligned} \mathcal{N}_\theta [\hat{\theta}(\xi, \eta; p), \hat{f}(\xi, \eta; p)] &= (1 + N_R) \frac{\partial^2 \hat{\theta}(\xi, \eta; p)}{\partial \eta^2} \\ &+ Pr(1 - \xi) \left(\frac{\eta}{2} \frac{\partial \hat{\theta}(\xi, \eta; p)}{\partial \eta} - \xi \frac{\partial \hat{\theta}(\xi, \eta; p)}{\partial \xi} \right) \quad (44) \\ &+ Pr \xi \hat{f}(\xi, \eta; p) \frac{\partial \hat{\theta}(\xi, \eta; p)}{\partial \eta}, \end{aligned}$$

$$\begin{aligned} \mathcal{N}_\phi [\hat{\phi}(\xi, \eta; p), \hat{f}(\xi, \eta; p)] &= \frac{\partial^2 \hat{\phi}(\xi, \eta; p)}{\partial \eta^2} \\ &+ Sc(1 - \xi) \left(\frac{\eta}{2} \frac{\partial \hat{\phi}(\xi, \eta; p)}{\partial \eta} - \xi \frac{\partial \hat{\phi}(\xi, \eta; p)}{\partial \xi} \right) \quad (45) \\ &+ Sc \xi \hat{f}(\xi, \eta; p) \frac{\partial \hat{\phi}(\xi, \eta; p)}{\partial \eta} - \gamma Sc \xi \hat{\phi}(\xi, \eta; p). \end{aligned}$$

Obviously, when $p = 0$ and $p = 1$ then

$$\hat{f}(\xi, \eta; 0) = f_0(\xi, \eta), \quad \hat{f}(\xi, \eta; 1) = f(\xi, \eta), \quad (46)$$

$$\hat{g}(\xi, \eta; 0) = g_0(\xi, \eta), \quad \hat{g}(\xi, \eta; 1) = g(\xi, \eta), \quad (47)$$

$$\hat{\theta}(\xi, \eta; 0) = \theta_0(\xi, \eta), \quad \hat{\theta}(\xi, \eta; 1) = \theta(\xi, \eta), \quad (48)$$

$$\hat{\phi}(\xi, \eta; 0) = \phi_0(\xi, \eta), \quad \hat{\phi}(\xi, \eta; 1) = \phi(\xi, \eta). \quad (49)$$

In view of Taylor series with respect to p , we have

$$\hat{f}(\xi, \eta; p) = f_0(\xi, \eta) + \sum_{m=1}^{\infty} f_m(\xi, \eta) p^m. \quad (50)$$

$$\hat{g}(\xi, \eta; p) = g_0(\xi, \eta) + \sum_{m=1}^{\infty} g_m(\xi, \eta) p^m, \quad (51)$$

$$\hat{\theta}(\xi, \eta; p) = \theta_0(\xi, \eta) + \sum_{m=1}^{\infty} \theta_m(\xi, \eta) p^m, \quad (52)$$

$$\hat{\phi}(\xi, \eta; p) = \phi_0(\xi, \eta) + \sum_{m=1}^{\infty} \phi_m(\xi, \eta) p^m, \quad (53)$$

$$\begin{aligned} f_m(\eta) &= \frac{1}{m!} \left. \frac{\partial^m f(\xi, \eta; p)}{\partial \eta^m} \right|_{p=0}, \\ g_m(\eta) &= \frac{1}{m!} \left. \frac{\partial^m g(\xi, \eta; p)}{\partial \eta^m} \right|_{p=0}, \\ \theta_m(\eta) &= \frac{1}{m!} \left. \frac{\partial^m \theta(\xi, \eta; p)}{\partial \eta^m} \right|_{p=0}, \\ \phi_m(\eta) &= \frac{1}{m!} \left. \frac{\partial^m \phi(\xi, \eta; p)}{\partial \eta^m} \right|_{p=0}. \end{aligned} \quad (54)$$

The auxiliary parameters are so properly chosen that series (50)–(53) converge at $p = 1$. Then we have

$$f(\xi, \eta) = f_0(\xi, \eta) + \sum_{m=1}^{\infty} f_m(\xi, \eta), \quad (55)$$

$$g(\xi, \eta) = g_0(\xi, \eta) + \sum_{m=1}^{\infty} g_m(\xi, \eta), \quad (56)$$

$$\theta(\xi, \eta) = \theta_0(\xi, \eta) + \sum_{m=1}^{\infty} \theta_m(\xi, \eta), \quad (57)$$

$$\phi(\xi, \eta) = \phi_0(\xi, \eta) + \sum_{m=1}^{\infty} \phi_m(\xi, \eta). \quad (58)$$

The resulting problems at the m th-order deformation are

$$\mathcal{L}_f[f_m(\xi, \eta) - \chi_m f_{m-1}(\xi, \eta)] = \hbar_f \mathcal{R}_m^f(\xi, \eta), \quad (59)$$

$$\mathcal{L}_g[g_m(\xi, \eta) - \chi_m g_{m-1}(\xi, \eta)] = \hbar_g \mathcal{R}_m^g(\xi, \eta), \quad (60)$$

$$\mathcal{L}_\theta[\theta_m(\xi, \eta) - \chi_m \theta_{m-1}(\xi, \eta)] = \hbar_\theta \mathcal{R}_m^\theta(\xi, \eta), \quad (61)$$

$$\mathcal{L}_\phi[\phi_m(\xi, \eta) - \chi_m \phi_{m-1}(\xi, \eta)] = \hbar_\phi \mathcal{R}_m^\phi(\xi, \eta), \quad (62)$$

$$\begin{aligned} f_m(\xi, 0) = 0, \quad f'_m(\xi, 0) = 0, \quad f'_m(\xi, \infty) = 0, \\ g_m(\xi, 0) = 0, \quad g_m(\xi, \infty) = 0, \quad g'_m(\xi, \infty) = 0, \\ \theta_m(\xi, 0) = 0, \quad \theta_m(\xi, \infty) = 0, \quad \phi_m(\xi, 0) = 0, \\ \phi_m(\xi, \infty) = 0, \end{aligned} \quad (63)$$

$$\begin{aligned} \mathcal{R}_m^f(\eta) &= (1 + K) f''_{m-1} + (1 - \xi) \left(\frac{\eta}{2} f''_{m-1} - \xi \frac{\partial f'_{m-1}}{\partial \xi} \right) \\ &+ \xi \left[\sum_{k=0}^{m-1} [f_k f''_{m-1-k} - f'_k f'_{m-1-k}] - M^2 f'_{m-1} \right] + K g'_{m-1}, \end{aligned} \quad (64)$$

$$\begin{aligned} \mathcal{R}_m^g(\eta) &= \left(1 + \frac{K}{2} \right) g''_{m-1} + (1 - \xi) \left(\frac{1}{2} g_{m-1} + \frac{\eta}{2} g'_{m-1} \right. \\ &\left. - \xi \frac{\partial g_{m-1}}{\partial \xi} \right) + \xi \left[\sum_{k=0}^{m-1} [f_k g'_{m-1-k} - g_k f'_{m-1-k}] \right], \end{aligned} \quad (65)$$

$$\begin{aligned} \mathcal{R}_m^\theta(\eta) &= (1 + N_R) \theta''_{m-1} - Pr(1 - \xi) \left(\frac{\eta}{2} \theta'_{m-1} \right. \\ &\left. - \xi \frac{\partial \theta_{m-1}}{\partial \xi} \right) + \xi Pr \sum_{k=0}^{m-1} [f_k \theta'_{m-1-k} + g_k \theta'_{m-1-k}], \end{aligned} \quad (66)$$

$$\begin{aligned} \mathcal{R}_m^\phi(\eta) &= \phi''_{m-1} - Sc(1 - \xi) \left(\frac{\eta}{2} \phi'_{m-1} - \xi \frac{\partial \phi_{m-1}}{\partial \xi} \right) \\ &+ \xi Sc \sum_{k=0}^{m-1} f_k \phi'_{m-1-k} - \gamma Sc \xi \phi_{m-1}, \end{aligned} \quad (67)$$

$$\chi_m = \begin{cases} 0, & m \leq 1, \\ 1, & m > 1. \end{cases} \quad (68)$$

The general solutions of (59)–(62) are

$$f_m(\xi, \eta) = f_m^*(\xi, \eta) + C_1 + C_2 \exp(\eta) + C_3 \exp(-\eta), \tag{69}$$

$$g_m(\xi, \eta) = g_m^*(\xi, \eta) + C_4 + C_5 \exp(\eta) + C_6 \exp(-\eta), \tag{70}$$

$$\theta_m(\xi, \eta) = \theta_m^*(\xi, \eta) + C_7 \exp(\eta) + C_8 \exp(-\eta), \tag{71}$$

$$\phi_m(\xi, \eta) = \phi_m^*(\xi, \eta) + C_9 \exp(\eta) + C_{10} \exp(-\eta), \tag{72}$$

in which $f_m^*(\xi, \eta)$, $g_m^*(\xi, \eta)$, $\theta_m^*(\xi, \eta)$, $\phi_m^*(\xi, \eta)$ are the particular solutions of the (59)–(62). Note that these equations can be solved by the Mathematica software one after the other in the order $m = 1, 2, 3, \dots$

4. Convergence of the Homotopy Solutions

Obviously, the series solutions (55)–(58) depend upon the non-zero auxiliary parameters \hbar_f , \hbar_g , \hbar_θ , and \hbar_ϕ which can adjust and control the convergence of the HAM solutions. In order to see the range for admissible values of \hbar_f , \hbar_g , \hbar_θ , and \hbar_ϕ , the \hbar -curves of the functions $f''(\xi, 0)$, $g'(\xi, 0)$, $\theta'(\xi, 0)$, and $\phi'(\xi, 0)$ are plotted for the 10th-order of approximations. It is noticed from Figure 1 that the range for the admissible values of \hbar_f , \hbar_g , \hbar_θ , and \hbar_ϕ are $-0.8 \leq \hbar_f \leq -0.3$, $-0.9 \leq \hbar_g \leq -0.2$, and $-0.8 \leq \hbar_g, \hbar_\phi \leq -0.3$. Furthermore, our computation shows that the series given by (55)–(58) converge in the whole region of η when $\hbar_f = \hbar_g = -0.7 = \hbar_\theta = \hbar_\phi$. Figure 1 shows \hbar -curves for velocity and concentration when $\xi = 0.5$.

5. Results and Discussion

The main interest here is to study the variations of material parameter K , Hartman number M , Prandtl number Pr , radiation parameter N_R , Schmidt number Sc , and chemical reaction parameter γ on the velocity components, concentration field, and skin friction coefficient. Figures 2–14 have been sketched for this purpose. Figures 2–7 display the effects of dimensionless time τ , material parameter K , and Hartman number M on the velocity component $f'(\eta, \xi)$ and skin-friction coefficient $\xi^{1/2} Re_x^{1/2} C_{fx}$. The variation of dimensionless time τ on the velocity component $f'(\eta, \xi)$ is shown in Figure 2. Clearly, the velocity component $f'(\eta, \xi)$ increases by increasing τ . Figure 3 gives the variations of M on the velocity component $f'(\eta, \xi)$. The velocity component $f'(\eta, \xi)$ is

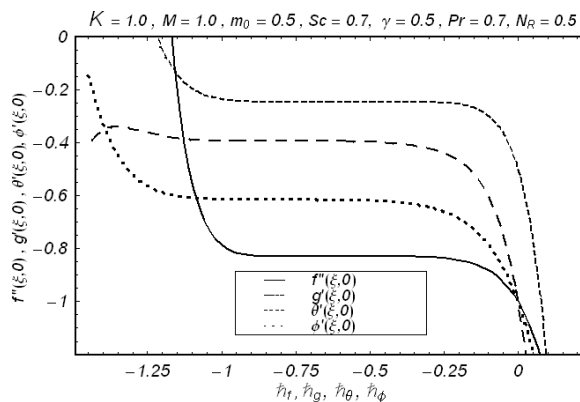


Fig. 1. \hbar -curves of $f''(\xi, 0)$, $g'(\xi, 0)$, $\theta'(\xi, 0)$, and $\phi'(\xi, 0)$ at 10th-order of approximations when $\xi = 0.5$.

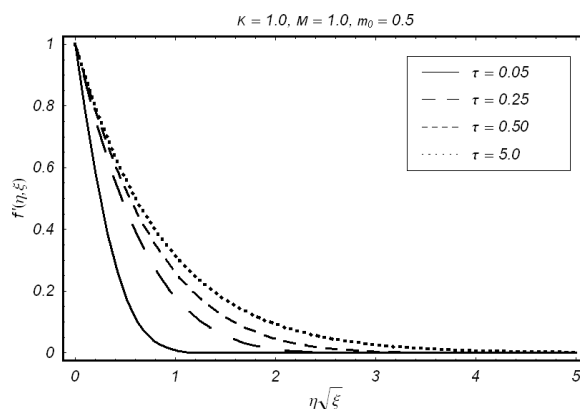


Fig. 2. Influence of τ on velocity profile f' .

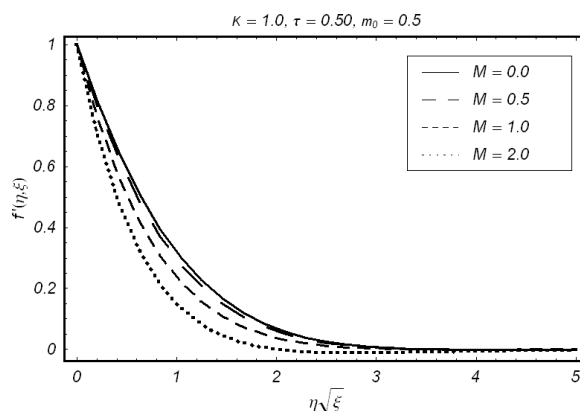


Fig. 3. Influence of M on velocity profile f' .

Table 1. Comparison of the values of skin friction coefficient $C_{fx}Re_x^{1/2}$ for values of K and m_0 when $M = 0$ and $\xi = 1$.

$K \setminus m_0$		0.0	0.5
0.0	[19]	-1.0000	-1.0000
	HAM	-1.000000	-1.000000
1.0	[19]	-1.3679	-1.2247
	HAM	-1.367872	-1.224741
2.0	[19]	-1.6213	-1.4142
	HAM	-1.621225	-1.414218
4.0	[19]	-2.0042	-1.7321
	HAM	-2.004133	-1.732052

Table 2. Values of skin friction coefficient $C_{fx}Re_x^{1/2}$ for various values of K and M when $\xi = 1$.

M	K	$C_{fx}Re_x^{1/2}$	$C_{fx}Re_x^{1/2}$
		$m_0 = 0.0$	$m_0 = 0.5$
0.0	1.0	-1.367872	-1.224754
		-1.530501	-1.363638
		-1.942227	-1.706493
1.0	0.0	-2.487393	-2.147621
		-1.118038	-1.118032
0.5	1.0	-1.530501	-1.363638
		-1.815277	-1.574471
		-2.245602	-1.929364
		-1.118038	-1.118032

a decreasing function of M . Figures 4 and 5 represent the velocity profiles for various values of K when $m_0 = 0.5$ and $m_0 = 0.0$, respectively. It is seen that results here are similar in both cases but the change in Figure 4 is slightly smaller when compared with Figure 5. The effects of K and M on the skin-friction coefficient $\xi^{1/2}Re_x^{1/2}C_{fx}$ are shown in the Figures 6 and 7. It is observed that the magnitude of skin friction coefficient $\xi^{1/2}Re_x^{1/2}C_{fx}$ increases when K and M are increased. Figures 8–11 are plotted for the microrotation profile $g(\eta, \xi)$. From Figures 10 and 11, one can observe that the microrotation profile for $m_0 = 0$ is different than for $m_0 = 0.5$.

Figures 12–14 are prepared for the effects of Prandtl number Pr , radiation parameter N_R , and dimensionless time τ on the temperature field $\theta(\eta, \xi)$. The variation of Pr on the temperature field is sketched in Figure 12. It is found that θ is a decreasing function of Pr . Figure 13 gives the effects of radiation parameter N_R on the temperature field. It has opposite results when compared with Figure 12. Figure 14 elucidates the influence of τ on $\theta(\eta, \xi)$. It is noticed that the temperature field $\theta(\eta, \xi)$ is an increasing function of τ and the concentration boundary layer thickness also increases for large values of τ . Figures 15–17 are prepared for the effects of dimensionless time τ , the Schmidt number Sc , and the chemical reaction parameter γ on the concentration field $\phi(\eta, \xi)$ and the sur-

Table 3. Values of $-\theta'(0)$ for some values of N_R , K , and Pr when $m_0 = 0.5$ and $\xi = 1$.

N_R	K	Pr	M	[16]	Present
1.0	1.0	1.0	0.0	0.3893	0.389321
	2.0			0.4115	0.411524
2.0	0.0			0.2588	0.259632
	1.0			0.2895	0.289547
	2.0			0.3099	0.309981
0.5	1.0	0.7	0.0	-	0.371412
			0.5	-	0.353991
	1.0			-	0.321648

Table 4. Values of $-\phi'(0)$ for some values of K , M , Sc , and γ when $m_0 = 0.5$ and $\xi = 1$.

Sc	γ	K	M	$-\phi'(0)$
0.5	1.0	1.0	0.5	0.820814
0.7				0.979971
1.2				1.299943
2.0				1.696172
0.5	1.0	1.0	0.5	0.820813
		2.0		1.088922
		3.0		1.301085
0.7	1.0	1.0	0.5	0.979971
		2.0		0.784003
		4.0		0.797627
0.7	1.0	1.0	0.0	0.781761
			0.5	0.773298
			1.0	0.754651
			1.5	0.734822

face mass transfer $\xi^{1/2}Re_x^{-1/2}C_{fx}Sh$. Figure 15 shows the influence of τ on the concentration field $\phi(\eta, \xi)$ in the case of destructive chemical reaction $\gamma > 0$. It is noted that concentration field $\phi(\eta, \xi)$ is an increasing function of τ and the concentration boundary layer thickness also increases for large values of τ . The variation of Sc on the concentration field is sketched in Figure 16. It is observed that ϕ is a decreasing function of Sc . Figure 17 gives the effects of destructive chemical reaction ($\gamma > 0$) on the concentration field. It is seen that results here are similar to $\gamma < 0$ but the change in Figure 17 is slightly smaller when compared with Figure 16. Figure 18 illustrates the variation of generative chemical reaction ($\gamma < 0$). It has opposite results when compared with Figure 17.

Tables 1–4 give the steady-state results ($\xi = 1$) for the surface shear stress, surface heat transfer, and surface mass transfer for different values of the emerging parameters. Table 1 includes the values of skin friction coefficient $C_{fx}Re_x^{1/2}$. This table indicates that the HAM solution is in good agreement with the numerical solution [30]. From Table 2 it is noticed that the magnitude of skin friction coefficient increases for large values of M and K . It is also observed from the comparison

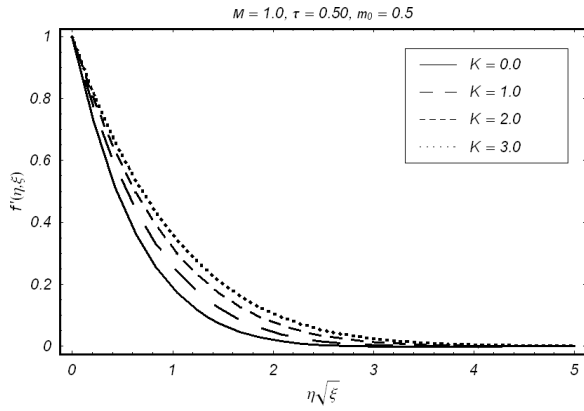


Fig. 4. Influence of K on velocity profile f' when $m_0 = 0.5$.

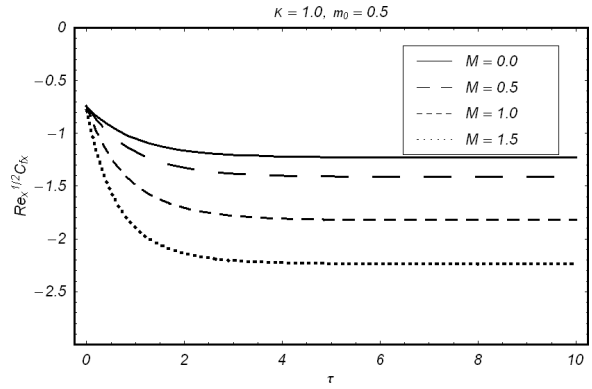


Fig. 7. Influence of M on $\xi^{1/2} Re_x^{1/2} Cf$.

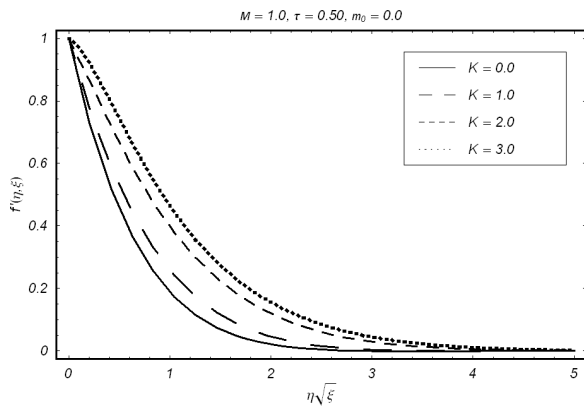


Fig. 5. Influence of K on velocity profile f' when $m_0 = 0.0$.

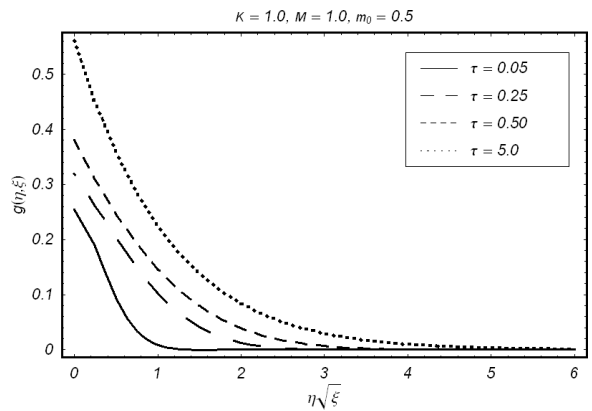


Fig. 8. Influence of τ on microrotation profile g when $m_0 = 0.5$.

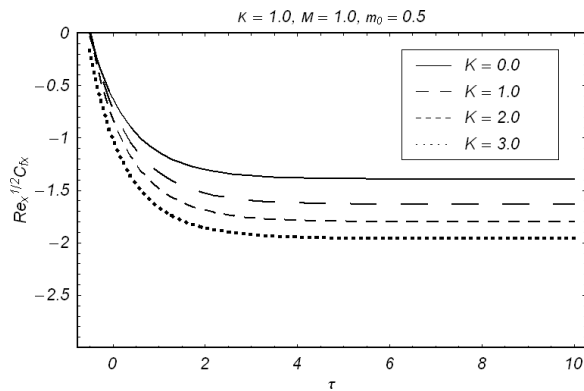


Fig. 6. Influence of K on $\xi^{1/2} Re_x^{1/2} Cf$.

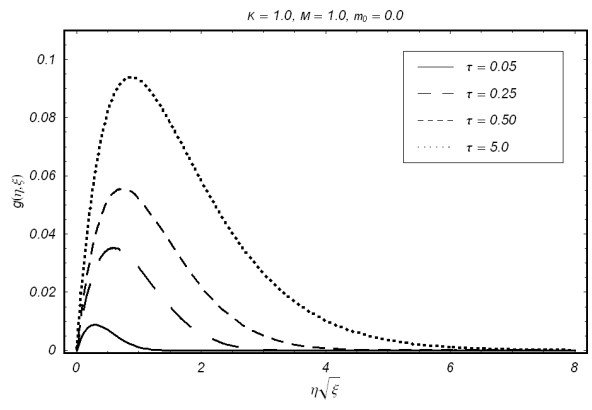


Fig. 9. Influence of τ on microrotation profile g when $m_0 = 0.0$.

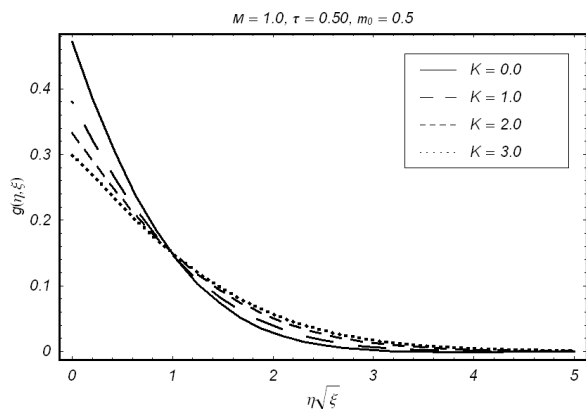


Fig. 10. Influence of K on microrotation profile g when $m_0 = 0.5$.

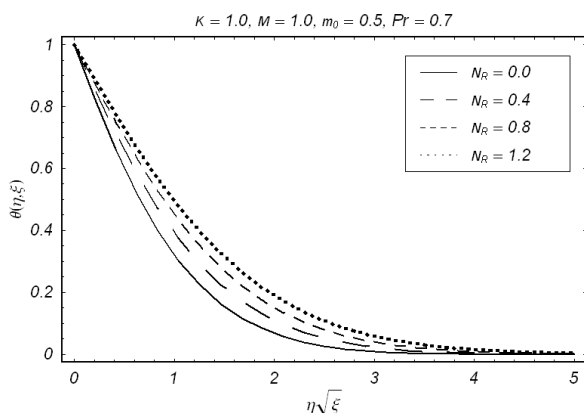


Fig. 13. Influence of N_R on temperature profile θ .

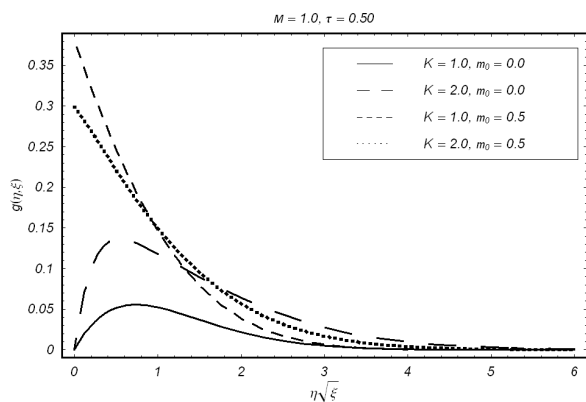


Fig. 11. Influence of K and m_0 on microrotation profile g .

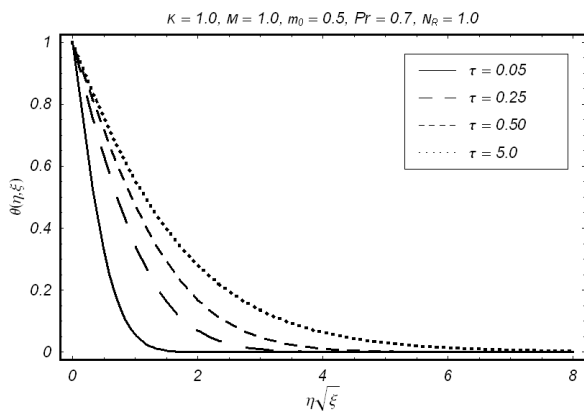


Fig. 14. Influence of τ on temperature profile θ .

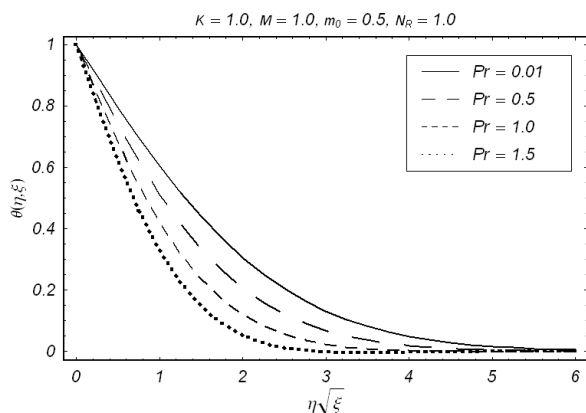


Fig. 12. Influence of Pr on temperature profile θ .

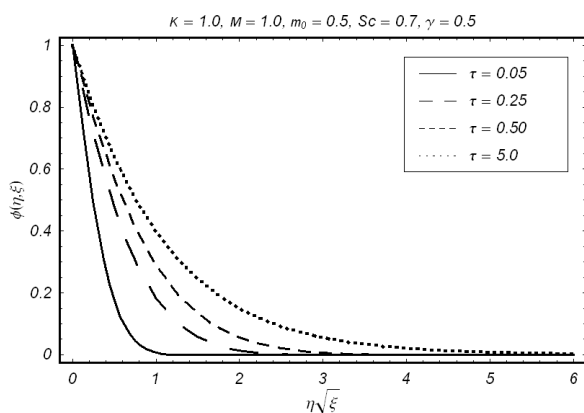


Fig. 15. Influence of τ on concentration profile ϕ .

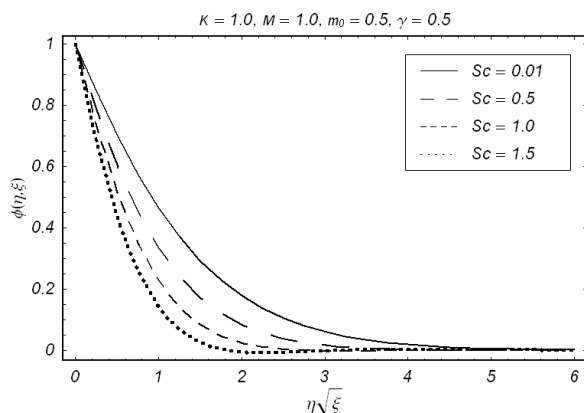


Fig. 16. Influence of Sc on concentration profile ϕ .

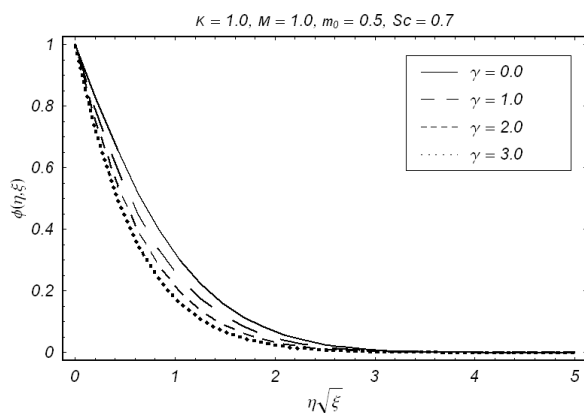


Fig. 17. Influence of $\gamma > 0$ on concentration profile ϕ .

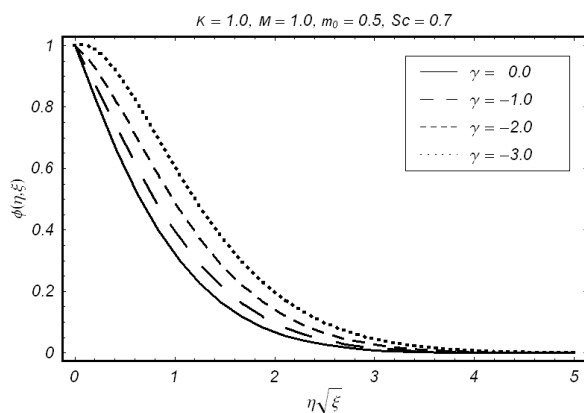


Fig. 18. Influence of $\gamma < 0$ on concentration profile ϕ .

of these tables that the magnitude of skin friction coefficient $C_{fx} Re_x^{1/2}$ is larger in the case of magnetohydrodynamic flow. Table 3 depicts the variation of the heat transfer characteristic at the wall $-\theta'(0)$ for different values of N_R , Pr , K , and M . The magnitude of $-\theta'(0)$ increases for larger values of K . Table 4 is prepared for the variation of K , M , Sc , and γ on the surface mass transfer. It is apparent from this table that the magnitude of $-\phi'(0)$ increases for large values of K and decreases for large values of M . The magnitude of $-\phi'(0)$ increases when Sc and γ are increased.

6. Closing Remarks

A mathematical model for the unsteady flow of a micropolar fluid with heat and mass transfer is presented. Computations for the nonlinear problems are made. The main results can be summarized as follows:

- The increasing values of M leads to a decrease in the boundary layer thickness.
- The fluid velocity increases as the microgyration parameter m_0 increases.
- Microrotation profile has a parabolic distribution for $m_0 = 0$.
- The temperature θ decreases when Pr increases.
- The variation of Pr on temperature is opposite to that of N_R .
- The influence of destructive chemical reaction parameter is to decrease the concentration field.
- The concentration field ϕ has opposite results for destructive ($\gamma > 0$) and generative ($\gamma < 0$) chemical reactions.
- The effects of Sc and destructive chemical reaction parameter ($\gamma > 0$) on the concentration field are opposite.

- [1] S. K. Jena and M. N. Mathur, *Int. J. Eng. Sci.* **19**, 1431 (1981).
- [2] G. S. Guram and A. C. Smith, *Comput. Math. Appl.* **6**, 213 (1980).
- [3] G. Ahmadi, *Int. J. Eng. Sci.* **14**, 639 (1976).
- [4] J. Peddieson, *Int. J. Eng. Sci.* **10**, 23 (1972).
- [5] C. Fetecau, C. Fetecau, M. Kamran, and D. Vieru, *J. Non-Newtonian Fluid Mech.* **156**, 189 (2009).
- [6] T. Hayat, Z. Abbas, and T. Javed, *Phys. Lett A* **372**, 637 (2008).
- [7] C. Fetecau and C. Fetecau, *Int. J. of Eng. Sci.* **44**, 788 (2006).
- [8] S. Asghar, T. Hayat, and P. D. Ariel, *Commun. Nonlinear Sci. Numer. Simul.* **14**, 154 (2009).
- [9] T. Hayat, I. Naeem, M. Ayub, A. M. Siddiqui, S. Asghar, and C. M. Khalique, *Nonlinear Analysis: Real World Appl.* **10**, 2117 (2009).
- [10] T. Hayat, Z. Abbas, and M. Sajid, *Phys. Lett. A* **372**, 2400 (2008).
- [11] Kh. S. Mekheimer and M. A. El Kot, *Acta Mech. Sin.* **24**, 637 (2008).
- [12] C. Fetecau and C. Fetecau, *Int. J. Eng. Sci.* **43**, 781 (2005).
- [13] P. D. Ariel, T. Hayat, and S. Asghar, *Acta Mech.* **187**, 29 (2006).
- [14] Kh. S. Mekheimer, *Phys. Lett. A* **372**, 4271 (2008).
- [15] M. Husain, T. Hayat, and C. Fetecau, *Nonlinear Analysis: Real World Appl.* **10**, 2133 (2009).
- [16] A. Ishak, *Meccanica*, DOI 10.1007/s11012-009-9257-4.
- [17] D. Pal, S. Chatterjee, *Commun. Nonlinear Sci. Numer. Simul.* **15**, 1843 (2010).
- [18] T. Hayat, M. Nawaz, M. Sajid, and S. Asghar, *Comput. Math. Appl.* **58**, 369 (2009).
- [19] R. Nazar, N. Amin, D. Filip, and I. Pop, *Int. J. Nonlinear Mech.* **39**, 1227 (2004).
- [20] H. S. Takhar, R. Bhargava, R. S. Agrawal, and A. V. S. Balaji, *Int. J. Eng. Sci.* **38**, 1907 (2000).
- [21] C. L. Chang, *J. Phys. D: Appl. Phys.* **39**, 1132 (2006).
- [22] R. S. R. Gorla, *Int. J. Eng. Sci.* **18**, 611 (1990).
- [23] E. M. Abo-Eldahab and M. A. E. Aziz, *Appl. Math. Comput.* **162**, 881 (2005).
- [24] T. K. V. Iyengar and V. G. Vani, *Int. J. Eng. Sci.* **42**, 1035 (2004).
- [25] D. Philip and P. Chandra, *Int. J. Eng. Sci.* **34**, 87 (1996).
- [26] D. A. S. Rees and A. P. Bassom, *Int. J. Eng. Sci.* **34**, 113 (1996).
- [27] T. Hayat, T. Javed, and Z. Abbas, *Nonlinear Analysis: Real World Appl.* **10**, 1514 (2009).
- [28] C. Y. Cheng, *Appl. Math. Model.* **34**, 1892 (2010).
- [29] N. T. Eldabe, M. E. M. Ouaf, *Appl. Math. Comput.* **177**, 561 (2006).
- [30] R. Nazar, A. Ishak, and I. Pop, *World Acadmey, Sci. Eng. & Tech.* **38**, 118 (2008).
- [31] S. J. Liao, *Beyond perturbation: Introduction to homotopy analysis method*, Chapman and Hall CRC Press, Boca Raton 2003.
- [32] S. J. Liao, *Appl. Math. Comput.* **147**, 499 (2004).
- [33] T. Hayat and Z. Abbas, *Z. Angew. Math. Phys.* **59**, 124 (2008).
- [34] S. Abbasbandy, *Chaos, Solitons, and Fractals* **39**, 428 (2009).
- [35] A. S. Bataineh, M. S. M. Noorani, and I. Hashim, *Phys. Lett. A* **372**, 613 (2008).
- [36] W. Wu and S. J. Liao, *Chaos, Solitons, and Fractals* **26**, 117 (2005).
- [37] T. Hayat, M. Qasim, and Z. Abbas, *Z. Naturforsch.* **64a**, 231 (2010).
- [38] A. S. Bataineh, M. S. M. Noorani, and I. Hashim, *Commun. Nonlinear Sci. Numer. Simul.* **14**, 409 (2009).
- [39] T. Hayat, M. Qasim, and Z. Abbas, *Int. J. Numer. Math. Fluids* 10.1002/flid.2252.
- [40] S. J. Liao, *Commun. Nonlinear Sci. Numer. Simul.* **14**, 2144 (2009).
- [41] S. J. Liao, *Commun. Nonlinear Sci. Numer. Simul.* **14**, 983 (2009).
- [42] T. Hayat, M. Qasim, and Z. Abbas, *Commun. Nonlinear Sci. Numer. Simul.* **15**, 2375 (2010).
- [43] S. Abbasbandy, *Chem. Eng. J.* **136**, 114 (2008).
- [44] S. J. Liao and Y. Tan, *Stud. Appl. Math.* **119**, 297 (2007).
- [45] Z. Abbas and T. Hayat, *Int. J. Heat Mass Transf.* **51**, 1024 (2008).
- [46] T. Hayat and M. Nawaz, *Int. J. Numer. Math. Fluids* 10.1002/flid.2251.
- [47] P. A. Davidson, *An introduction to magnetohydrodynamics*, Cambridge University Press, Cambridge 2001.